Supporting Information

1. Experimental section

Synthesis of $[Au_{28}Cu_{12}(SR)_{24}](PPh_4)_4$

20 mg CuCl dissolved in mixture of 10 mL tetrahydrofuran and 10 mL dichloromethane and stirred vigorously. After CuCl was fully dissolved, 32 mg triphenylphosphine-triphenylborane and 30 μL $C_6H_4Cl_2S$ (2,4-dichlorothiophenol) were added successively. When the solution turned clear light yellow, 27 mg Me_2SAu was added. After stirring for 10 minutes, 30 mg $NaBH_4$ in 1 mL cold water was dropwise added. The reaction was carried out at room temperature for 4 hours. The crude products were separated and purified by thin layer chromatography with dichloromethane/petroleum ether as developing agent. Finally, n-hexane was diffused into a solution of acetone for a week to obtain Dark green flake crystals.

Synthesis of $Au_{28}(TBBT)_{20}$

$Au_{28}(TBBT)_{20}$ (TBBT=4-tert-butylbenzenethiol) was synthesized based on the reported literature.[S1,S2] Firstly, 500 mg $HAuCl_4 \cdot 4H_2O$ and 675 mg TOAB were dissolved in 35 mL tetrahydrofuran, and 1020 μL 2-phenylethanethiol (2-phenylethanethiol=PET) was added under stirring. After the solution became colorless and transparent, 538 mg $NaBH_4$ in 8ml cold water was quickly added. The reaction was carried out at 0 ℃ overnight, and then the product was washed with methanol and extracted with toluene to obtain $Au_{25}(PET)_{18}$. Secondly, 10 mg $Au_{25}(PET)_{18}$ and 500 μL 4-tert-butylbenzenethiol was added in 500 μL toluene, the solution was stirring at 80 ℃ oil bath for 2 hours. Finally, the product was washed with methanol and purified by thin-layer chromatography to obtained $Au_{28}(TBBT)_{20}$.

Synthesis of $Cu_{28}(CHT)_{18}(PPh_3)_3$

100 mg $Cu(MeCN)_4BF_4$ and 80 mg PPh_3 dissolved in mixture of 4 mL acetonitrile and 1 mL dichloromethane. 30 μL CHT (cyclohexanethiol) was added after the solution turned colorless and transparent. After stirring for 20 minutes, solution turned turbid and 100 mg $NaBH_4$ in 5 mL methanol was added immediately. The reaction

was carried out at room temperature for 3 hours. The reaction mixture was centrifuged and the precipitates were washed with methanol and n-hexane successively to obtain the crude product. Finally, n-hexane was diffused into a solution of dichloromethane for a week to obtain red crystals.

Electrochemical measurement

All electrochemical tests were carried in a customized H-type electrolytic cell, in which the anode and cathode compartments were separated by a Nafion 117 membrane. The clusters uniformly coated on 1 cm×cm carbon paper (Toray TGP-H-060) were used as the working electrode, to be specific, ~1 mg clusters were dissolved in 500 μL dichloromethane, the solution was dropped on 1 cm×cm carbon paper which was fixed in platinum electrode clamp. Ag/AgCl (saturated KCl aqueous solution) electrode and platinum sheet electrode were respectively used as reference electrode and counter electrode. All tests for NRA were performed on the electrochemical workstation of Shanghai Chenhua CHI660D. All the electrode potentials in this study were converted to the reversible hydrogen electrode potential (RHE) through $E_{RHE} = E_{Ag/AgCl} + 0.198\ V + 0.059 \times pH$. Before the electrochemical measurements, pure Ar gas was injected into 0.05M H_2SO_4 with or without 0.5 M NO_3^- electrolytes for 30 mins to remove oxygen and nitrogen, and then electrodes were activated by implementing cyclic voltammetry (CV) tests at a scan rate of 50 mV/s from +0.25 V to -1.15 V vs. RHE for 50 cycles. The linear voltammetry curve (LSV) was measured at a scanning rate of 10 mV/s from -0.15 V to −1.15 V vs RHE at room temperature. Chronoamperometry test was performed at different potentials for 2 h and the electrolytes were collected to calculate the Faraday efficiency and yield rate of NH_3. During the chronoamperometry test, the electrolyte in the cathode region was stirred at a speed of 600 rpm, and Ar gas was continuously injected to purify it. The electrochemical impedance spectroscopy (EIS) was performed at 0 V vs. RHE from 10^5 to 10^{-2} Hz. The electrochemcial active surface area (ECSA) was measured by double layer capacitance method: Firstly, CV curves of clusters were tested at scan rates of 0.02, 0.06, 0.10, 0.14 and 0.18 V/s from 0.10 to 0.30 V vs RHE. Then the linear fitting of CV curve area under different scan speed was carried out,

and the slope of the fitting line was the double electric layer capacitance which can reflected the value of ECSA.

Characterization

The UV−vis spectra were characterized by a Shimadzu UV-1800 UV-vis spectrometer. The single crystal X-ray diffraction data of $[Au_{28}Cu_{12}(SR)_{24}](PPh_4)_4$ were collected on a Bruker D8 VENTURE with Mo Kα radiation (λ = 0.71073 Å) at 296.2 K. The single crystal X-ray diffraction data of $Cu_{28}(CHT)_{18}(PPh_3)_3$ were collected on a Bruker D8 VENTURE with Cu Kα radiation (λ = 1.54178 Å) at 193.2 K. Electrospray ionization (ESI) mass spectra of $Au_{28}(DMPA)_{20}$ were collected using a Z spray source on a Waters Q-TOF mass spectrometer. The cluster sample was dissolved in toluene (0.5 mg/mL) and then the solution was diluted with methanol solution containing 50 mmol/L Cs_2CO_3 (2:1 V/V). The liquid products were determined by ^1H NMR on BRUKER AVANCE III 400 MHz with Dimethyl sulfoxide (DMSO) as internal standard.

Determination of H_2 and N_2

During the reaction, the electrolyte in the cathode region was stirred at a speed of 600 rpm, and Ar gas was continuously injected at a gas flow rate of 18 mL/min. Every 100 minutes, the exhaust gas from the cathode region was analyzed by a gas chromatograph equipped with a thermal conductivity detector (TCD).

Determination of NH_3-N concentration by ^1H NMR

9 mL electrolyte after the reaction, 1 mL D_2O and 1 μL DMSO (internal standard) were added into glass bottle. After mixing evenly, 500 μL solution was added into the nuclear magnetic tube, which was tested by BRUKER AVANCE III 400 MHz at ambient condition.

Determination of ion concentration by colorimetry

Determination of NH_3-N: NH_3-N was determined using Nessler's reagent as the color reagent. 5 μL electrolyte after the reaction was diluted to 5 mL, 10 μL 5 M NaOH aqueous solution was added to adjust the pH. 120 μL potassium sodium tartrate solution (ρ = 500 g/L) was added and mixed thoroughly, then 150 μL Nessler's

reagent was added. The absorption intensity at a wavelength of 420 nm was recorded after sitting for 10 min.

Determination of NO_2^--N: A mixture of *p*-aminobenzenesulfonamide (4 g), N-(1-Naphthyl) ethylenediamine dihydrochloride (0.2 g), ultrapure water (50 mL) and phosphoric acid (10 mL, ρ = 1.70 g/mL) was used as a color reagent. 100 μL color reagent was added into 5 mL electrolyte and mixed uniformity. The absorption intensity at a wavelength of 540 nm was recorded after sitting for 10 min.

Determination of N_2H_4-N: Watt-Chrisps methods were used to detect the content of N_2H_4. The mixture of 4-Dimethylaminobenzaldehyde (4 g), concentrated HCl (20 mL) and ethanol (200 mL) is the color reagent.5 mL color reagent was added into 5 mL electrolyte and mixed uniformity. The absorption intensity at a wavelength of 458 nm was recorded after sitting for 10 min.

2. Supporting Figures and Tables

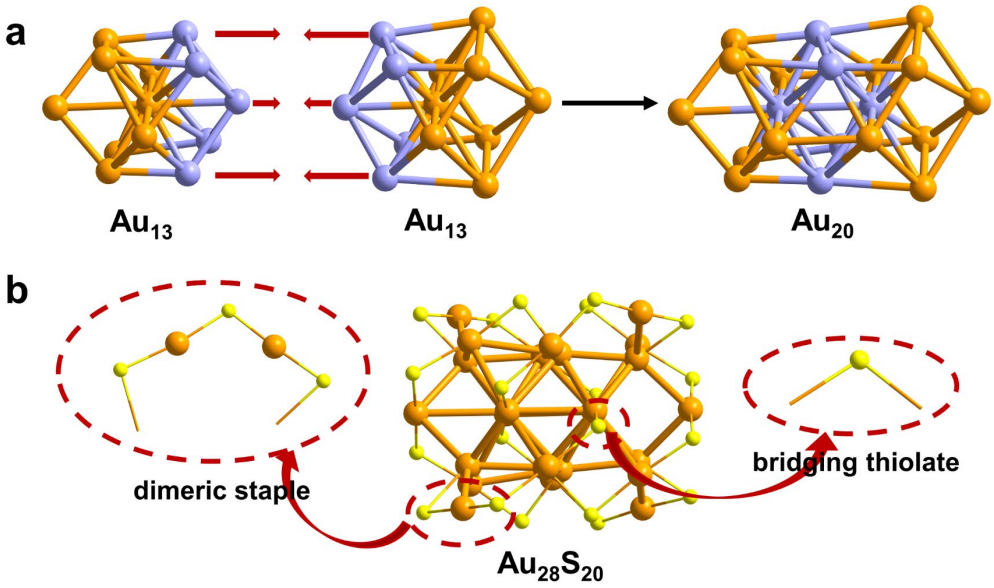

Figure S1. (a) Au_{20} core of $Au_{28}(TBBT)_{20}$. (b) Dimeric staples $Au_2(TBBT)_3$ and bridging thiolates of $Au_{28}(TBBT)_{20}$. Color code: orange/purple, Au; yellow: S. The C and H atoms are omitted for clarity.

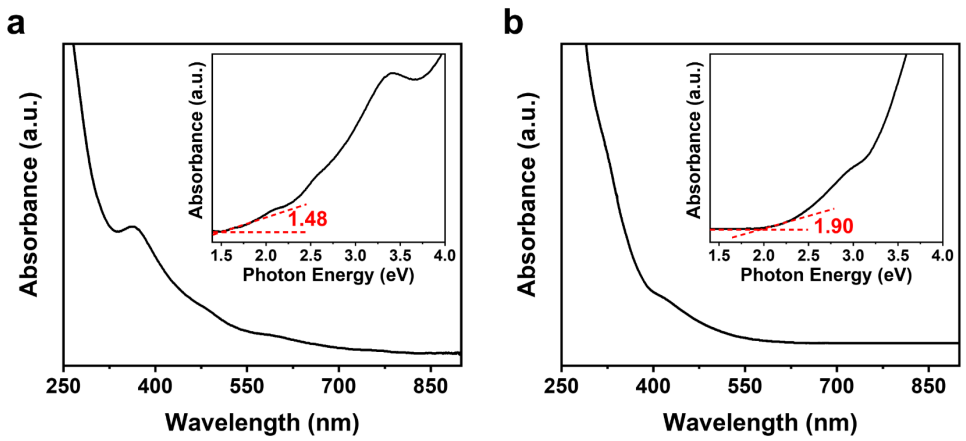

Figure S2. UV-vis spectra of (a) $Au_{28}(TBBT)_{20}$ and (b) $Cu_{28}(CHT)_{18}(PPh_3)_3$. The insets are the corresponding the photon energy scales.

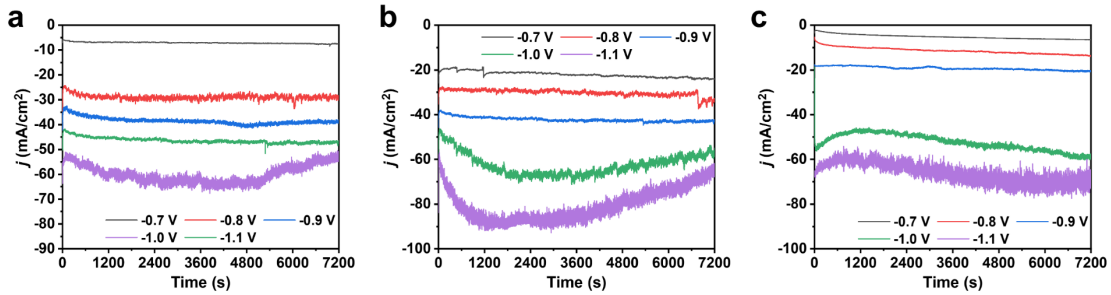

Figure S3. I-t curves of (a) $Au_{28}Cu_{12}$, (b) Au_{28} and (c) Cu_{28} from -0.7 to -1.1 V vs. RHE in 0.05 M H_2SO_4 electrolyte with 0.5 M KNO_3.

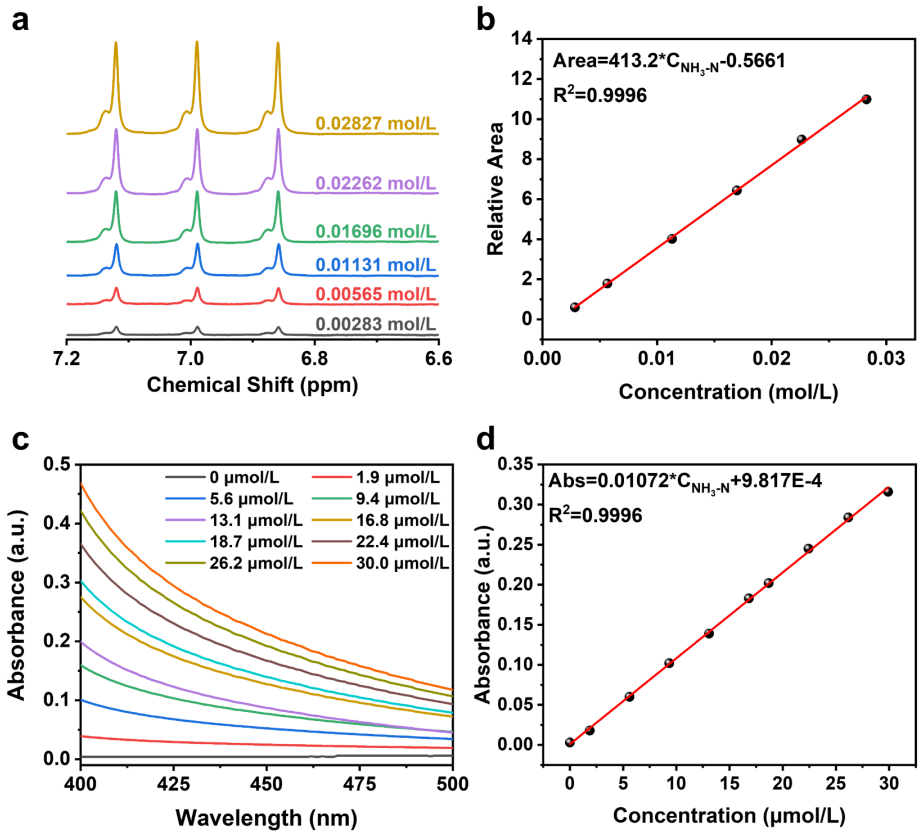

Figure S4. (a) ^{1}H NMR spectra and (c) UV-vis spectra of NH_4^+. The standard curves of NH_3-N concentration obtained by (b) ^{1}H NMR and (d) Nessler's reagent spectrophotometry.

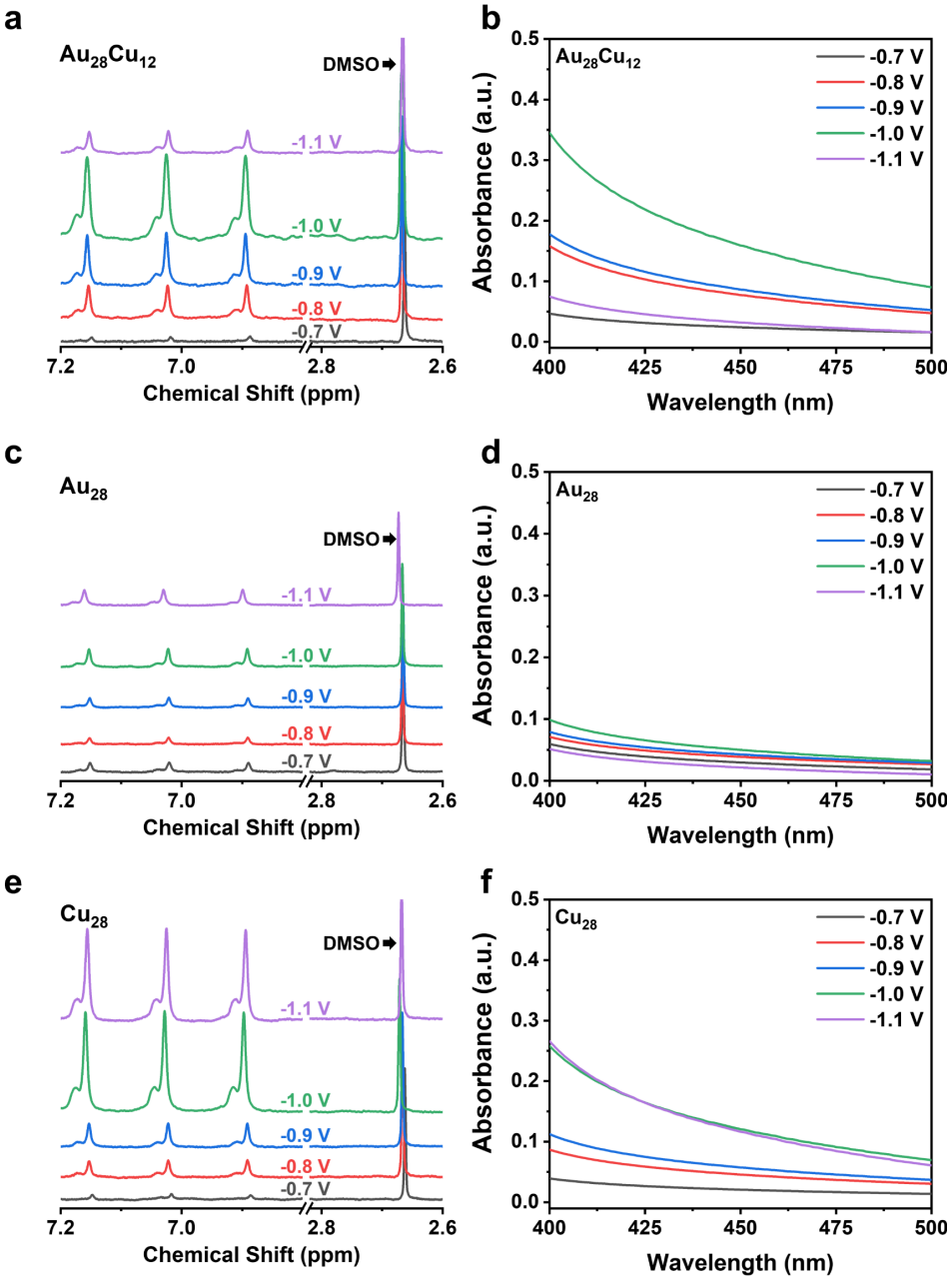

Figure S5. ^{1}H NMR spectra to measure NH_4^+ of electrolytes after the I-t tests obtained by different electrolytic conditions over (a) $Au_{28}Cu_{12}$, (c) Au_{28} and (e) Cu_{28}, respectively. UV-vis spectra to measure NH_4^+ of electrolytes after the I-t tests obtained by different electrolytic conditions over (b) $Au_{28}Cu_{12}$, (d) Au_{28} and (f) Cu_{28}, respectively.

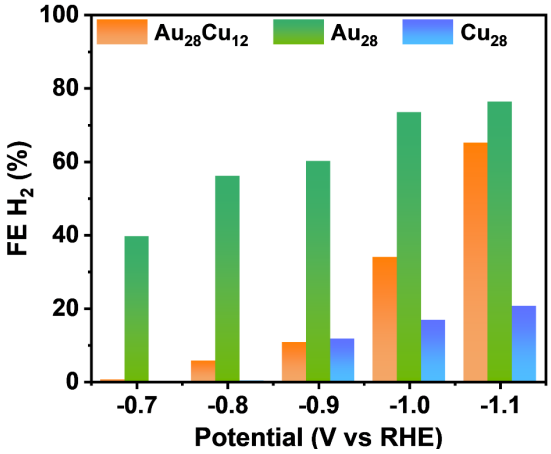

Figure S6. Potential-dependent H_2 faradaic efficiency of $Au_{28}Cu_{12}$, Au_{28} and Cu_{28} in 0.05 M H_2SO_4 electrolyte with 0.5 M KNO_3.

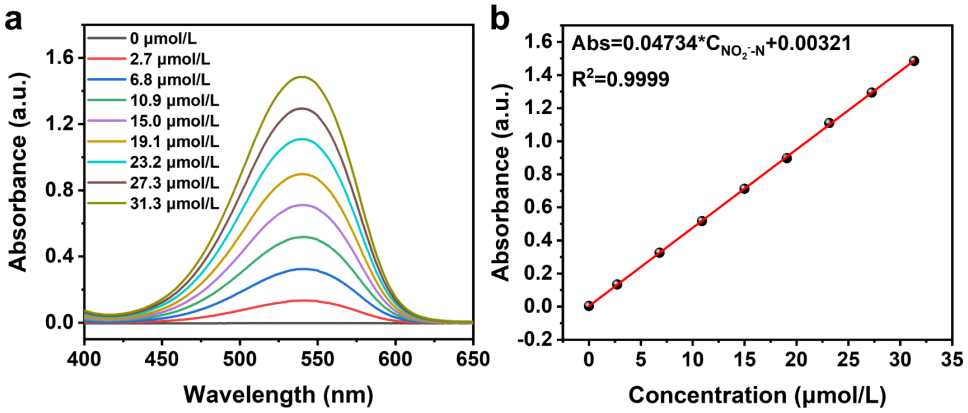

Figure S7. (a) UV-vis spectra of NO_2^-. (b) The standard curve of NO_2^--N concentration obtained by colorimetry.

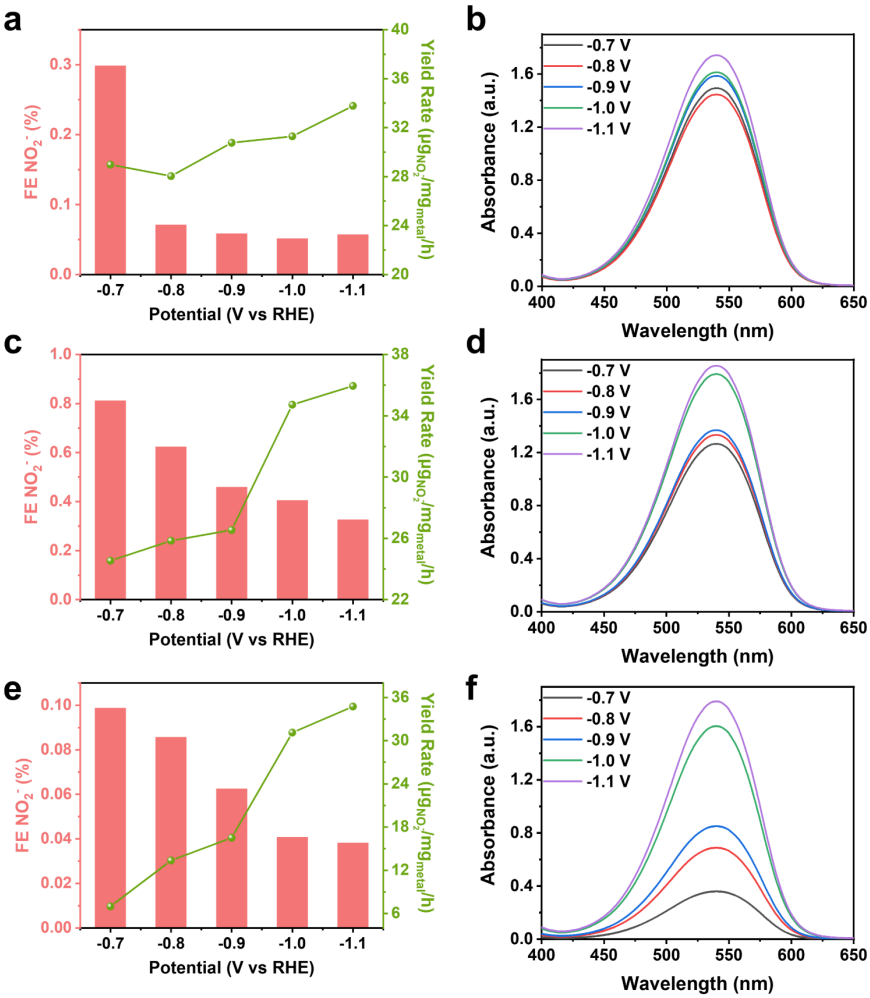

Figure S8. FEs and yield rates of NO_2^- over (a) $Au_{28}Cu_{12}$, (c) Au_{28} and (e) Cu_{28} clusters, respectively. UV-vis absorption spectra to measure NO_2^- of electrolytes after the I-t tests obtained by different electrolytic conditions over (b) $Au_{28}Cu_{12}$, (d) Au_{28} and (f) Cu_{28} clusters.

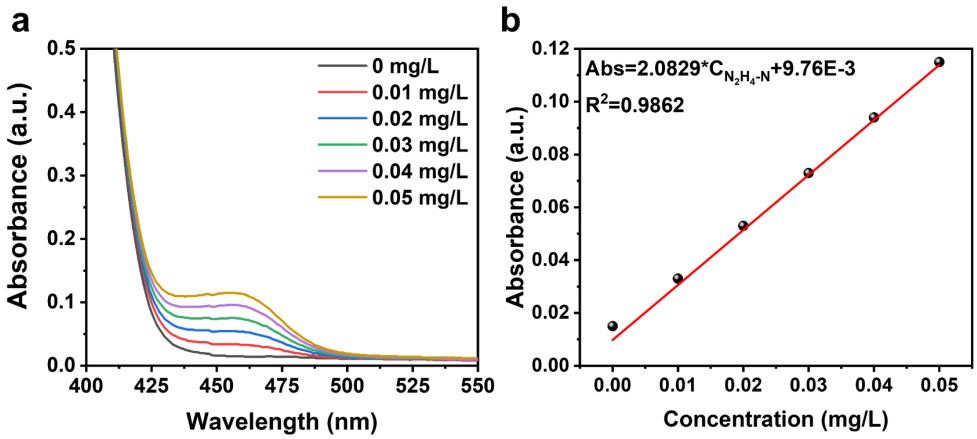

Figure S9. (a) UV-vis absorption spectra of N_2H_4. (b) The standard curve of N_2H_4-N concentration obtained by colorimetry.

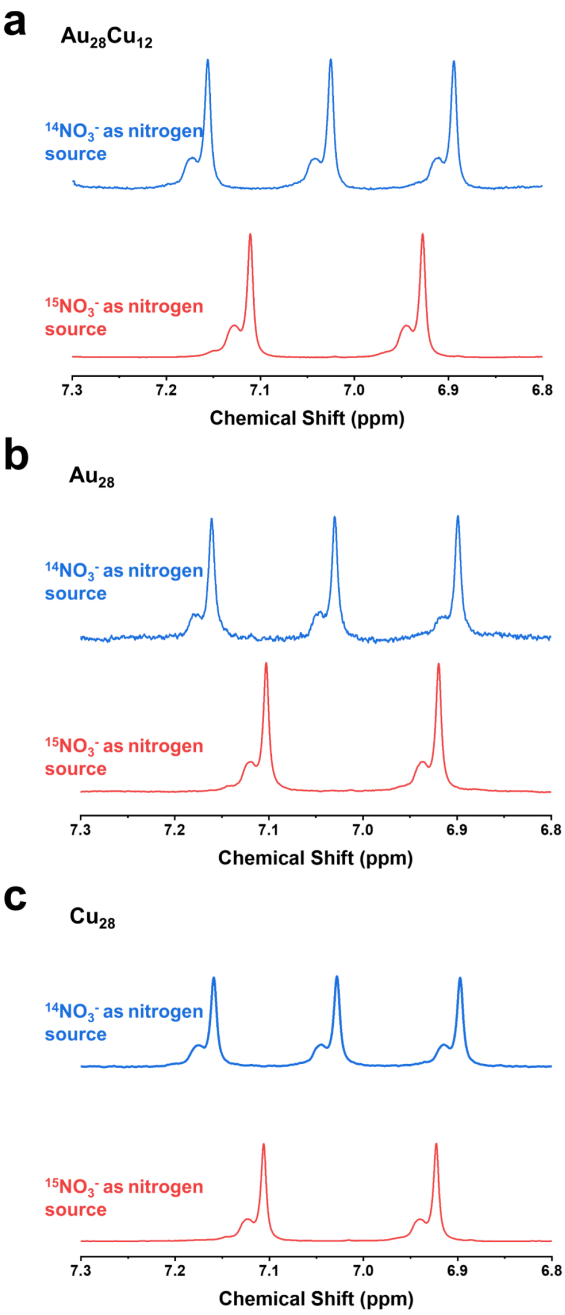

Figure S10. ^{1}H NMR spectra of the products generated after electrocatalytic NRA reaction in 0.05 M H_2SO_4 electrolyte with 0.5 M $^{14}NO_3^-$ and $^{15}NO_3^-$ at -0.8 V vs RHE over (a) $Au_{28}Cu_{12}$, (b) Au_{28} and (c) Cu_{28}.

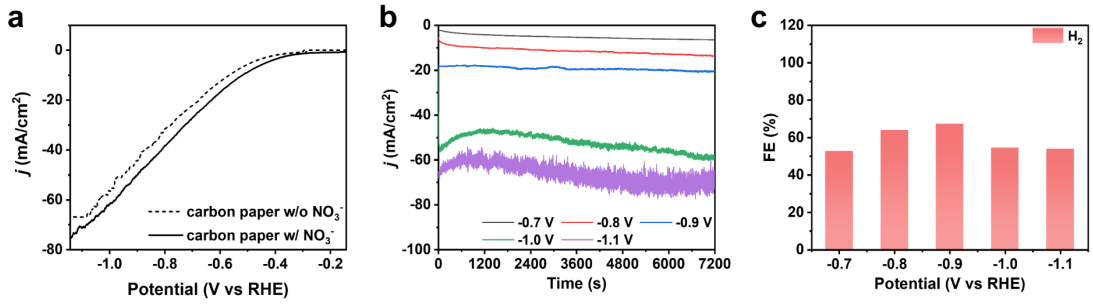

Figure S11. (a) LSV curves of carbon paper in 0.05 M H_2SO_4 electrolyte with or without NO_3^-. (b) I-t curves of carbon paper from -0.7 to -1.1 V. (c) H_2 FEs over carbon paper. RHE in 0.05 M H_2SO_4 electrolyte with 0.5 M KNO_3.

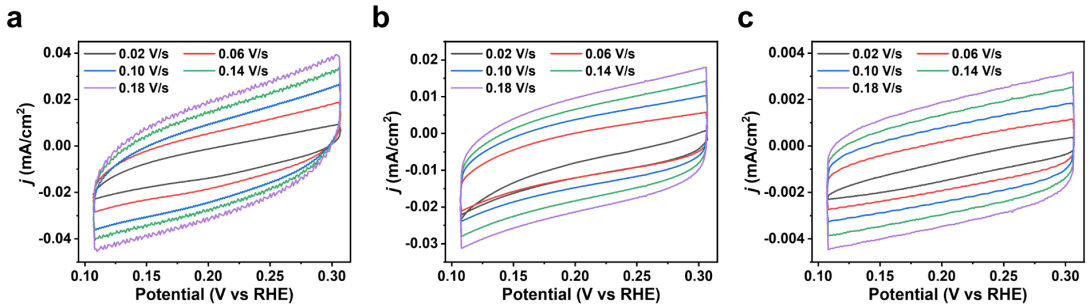

Figure S12. The CV curves in the non-faradaic region of (a) $Au_{28}Cu_{12}$, (b) Au_{28} and (c) Cu_{28} clusters, respectively.

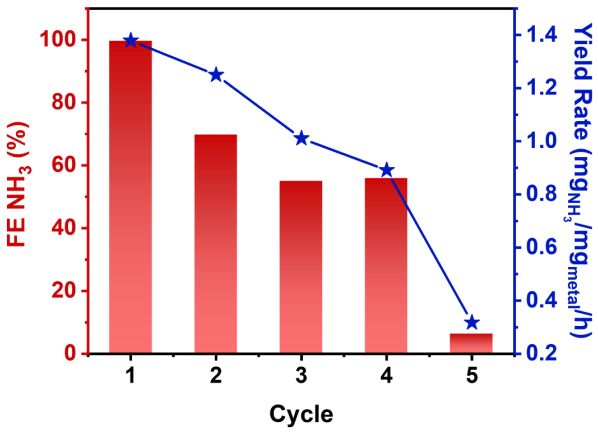

Figure S13. Recycling test at -0.8 V vs RHE of the Cu_{28} cluster.

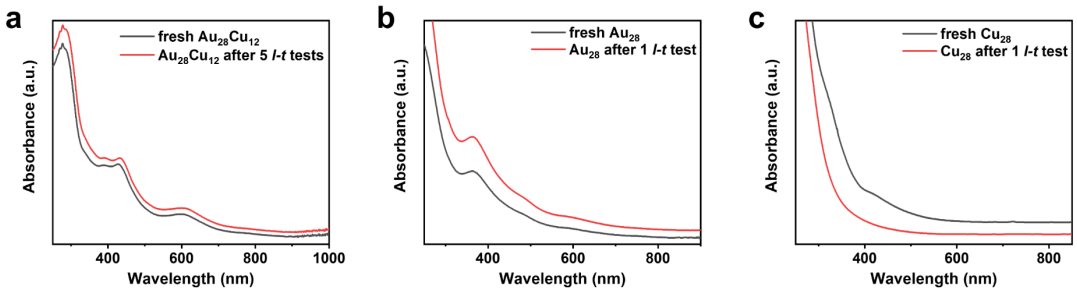

Figure S14. UV-vis spectra of the clusters before and after *I-t* tests at -0.8 V: (a) $Au_{28}Cu_{12}$, (b) Au_{28} and (c) Cu_{28} clusters. (The spent clusters were dissolved from carbon paper by dichloromethane.)

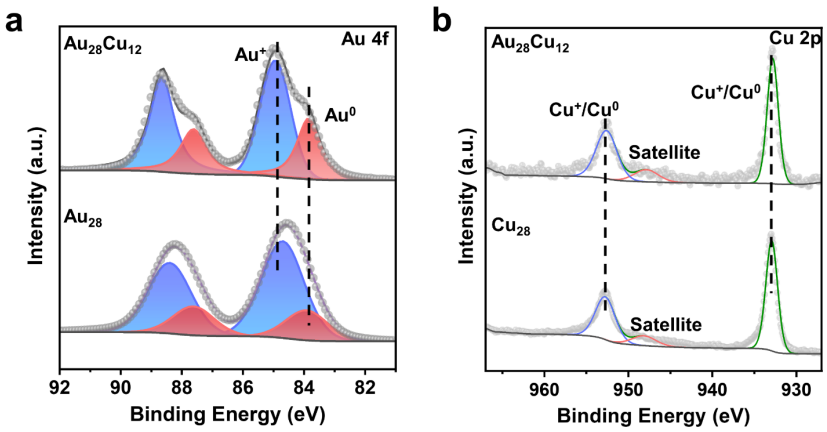

Figure S15. XPS profiles of the spent clusters after *I-t* tests at -0.8 V: (a) Au 4f XPS profiles; (b) Cu 2p XPS profiles.

Table S1. Binding energy values of Au species and their relative quantities in the $Au_{28}Cu_{12}$ and Au_{28} clusters.

Sample	Binding energy of Au species (eV)				Relative amount of Au species	
	Au $4f_{5/2}$		Au $4f_{7/2}$		Au^0	Au^+
	Au^0	Au^+	Au^0	Au^+		
$Au_{28}Cu_{12}$	87.6	88.5	83.9	84.8	39.68%	60.32%
Au_{28}	87.6	88.5	83.9	84.8	21.84%	78.16%

Table S2. Crystal data and structure refinement for the $[Au_{28}Cu_{12}(SR)_{24}](PPh_4)_4$ cluster.

Empirical formula	C240H152Au28Cl48Cu12P4S24	
Formula weight	11908.07	
Temperature	296(2) K	
Wavelength	0.71073 Å	
Crystal system	Triclinic	
Space group	P-1	
Unit cell dimensions	a = 22.0728(13) Å	a= 86.596(2)°.
	b = 27.5087(14) Å	b= 78.050(2)°.
	c = 27.5493(15) Å	g = 88.550(2)°.
Volume	16334.9(16) $Å^3$	
Z	2	
Density (calculated)	2.421 Mg/m^3	
Absorption coefficient	13.884 mm^{-1}	
F(000)	10824	
Theta range for data collection	1.998 to 25.027°.	
Index ranges	-20<=h<=26, -32<=k<=32, -32<=l<=32	
Reflections collected	119291	
Completeness to theta = 25.027°	99.4 %	
Refinement method	Full-matrix least-squares on F^2	
Data / restraints / parameters	57407 / 8160 / 3013	
Goodness-of-fit on F^2	1.212	
Final R indices [I>2sigma(I)]	R1 = 0.0907, wR2 = 0.2200	
R indices (all data)	R1 = 0.1293, wR2 = 0.2435	
Extinction coefficient	n/a	
Largest diff. peak and hole	7.198 and -7.207 $e.Å^{-3}$	

Table S3. Crystal data and structure refinement for the $Cu_{28}(CHT)_{18}(PPh_3)_3$ cluster.

Empirical formula	C162H243Cu28P3S18	
Formula weight	4639.66	
Temperature	193(2) K	
Wavelength	1.54178 Å	
Crystal system	Monoclinic	
Space group	$P2_1/n$	
Unit cell dimensions	a = 19.6220(11) Å	a= 90°.
	b = 39.5629(18) Å	b= 91.255(3)°.
	c = 26.1094(12) Å	g = 90°.
Volume	20264.0(17) $Å^3$	
Z	4	
Density (calculated)	1.521 Mg/m^3	
Absorption coefficient	5.310 mm^{-1}	
F(000)	9440	
Theta range for data collection	3.059 to 68.568°.	
Index ranges	-23<=h<=23, 0<=k<=47, 0<=l<=31	
Reflections collected	36264	
Completeness to theta = 67.679°	94.1 %	
Refinement method	Full-matrix least-squares on F^2	
Data / restraints / parameters	36264 / 4330 / 1826	
Goodness-of-fit on F^2	0.985	
Final R indices [I>2sigma(I)]	R1 = 0.1083, wR2 = 0.2575	
R indices (all data)	R1 = 0.1626, wR2 = 0.2931	
Extinction coefficient	n/a	
Largest diff. peak and hole	1.300 and -0.736 $e.Å^{-3}$	

Table S4. Comparison of ammonia selectivity by electrocatalytic nitrate reduction.

Electrocatalyst	Electrolyte	NO_3^- efficiency	Reference
$Au_{28}Cu_{12}$	0.5 M KNO_3+0.05 M H_2SO_4	97%	This work
Au_{28}	0.5 M KNO_3+0.05 M H_2SO_4	41%	This work
Cu_{28}	0.5 M KNO_3+0.05 M H_2SO_4	99.8%	This work
Au/Cu SAAs	100 ppm NO_3^-+0.5 M Na_2SO_4	98.3%	S3
Cu/Cu_2O	200 ppm NO_3^- + 0.5 M Na_2SO_4	97%	S4
Cu/GO/Ti	50 ppm NO_3^- + 0.05 M Na_2SO_4	91.5%	S5
para-MBA-Au/C	1.0 M KOH + 0.1 MKNO_3	98.7%	S6
Au-NC/TiO_2	0.2 M Na_2SO_4 + 0.05 M $NaNO_3$	91%	S7

3. Supporting references

S1 Z. Wu, J. Suhan and R. Jin, *J. Mater. Chem.*, 2009, **19**, 622-626.

S2 C. Zeng, Y. Chen, K. Iida, K. Nobusada, K. Kirschbaum, K. J. Lambright and R. Jin, *J. Am. Chem. Soc.,* 2016, **138**, 3950-3953.

S3 H. Yin, Y. Peng and J. Li, *Environ. Sci. Technol.*, 2023, **57**, 3134-3144.

S4 Y. Wang, W. Zhou, R. Jia, Y. Yu and B. Zhang, *Angew. Chem. Int. Ed. Engl.*, 2020, **59**, 5350-5354.

S5 J. Wang, S. Wang, Z. Zhang and C. Wang, *J. Environ. Manage.*, 2020, **276**, 111357.

S6 Y. Wu, X. Kong, Y. Su, J. Zhao, Y. Ma, T. Ji, D. Wu, J. Meng, Y. Liu, Z. Geng and J. Zeng, *Precis. Chem.*, 2024, **2**, 112-119.

S7 M. Yang, T. Wei, J. He, Q. Liu, L. Feng, H. Li, J. Luo and X. Liu, *Nano Res.*, 2024, **17**, 1209-1216.